International Research Journal on Advanced Engineering and Management
https://goldncloudpublications.com
https://doi.org/10.47392/IRJAEM.2026.0390
e ISSN: 2584-2854
Volume: 04 Issue: 08
August 2026
Page No: 2741 - 2754

Deformation Due To a Dip–Slip Fault At 45° In Dislocation–Like Imperfectly Bonded Elastic Half–Spaces

Meenal Malik[1]
[1]*Assistant Professor, Mathematics, All India Jat Heroes' Memorial College, Rohtak, Haryana*
Email: *meenaljalaj@gmail.com*[1]

Abstract
Closed-form analytical expressions for the displacements and stresses caused by a two-dimensional line source in two homogeneous, isotropic elastic half-spaces with imperfect bonding are derived using a dislocation-like interface model. In this model, the tractions are transmitted continuously across the interface, while the displacements may exhibit a discontinuity. As a special case, the deformation field associated with a dip-slip fault dipping at 45° is obtained in closed form. The effects of perfect and several imperfect bonding conditions on the dimensionless displacements and stresses are illustrated using line graphs, discontinuity plots, and three-dimensional mesh-grid maps with contour lines. The results show that imperfect bonding introduces a jump in displacement across the interface and substantially alters the surrounding deformation field. For the considered source, the vertical displacement is symmetric about the fault, whereas the horizontal displacement is antisymmetric. This behaviour is opposite to that observed for the vertical dip-slip case.
Keywords: *Deformation; Dip–slip fault; 45° dip; Dislocation–like interface; Imperfect bonding; Mesh grids; Contours.*

1. Introduction

The study of static deformation produced by seismic sources is important in seismology, geophysics, tectonophysics, and earthquake engineering. Understanding how the ground deforms during and after faulting helps in interpreting coseismic and interseismic ground movements, analysing stress transfer between faults, and assessing seismic hazards. The mathematical treatment of such deformation problems has its roots in the classical theory of elastic dislocations developed by Steketee (1958), Chinnery (1961), and Maruyama (1964). Subsequently, Savage (1966) and Freund and Barnett (1976) investigated surface deformation associated with dip-slip faulting, while Okada (1985) developed the widely used closed-form expressions for surface deformation caused by shear and tensile faults in a homogeneous half-space. The Earth's crust, however, is not a single homogeneous medium. It consists of different geological layers and materials that are separated by interfaces. Therefore, modelling the Earth as two elastic media in contact provides a more realistic representation of many geophysical situations. The fundamental solution for a point force in a semi-infinite solid was obtained by Mindlin (1936), while Rongved (1955) extended the formulation to two welded half-spaces. Dundurs and Hetényi (1965) further examined the transmission of force across a smooth interface. Heaton and Heaton (1989) studied static deformation produced by point forces and force couples in two welded Poissonian half-spaces. Their results showed an interesting dependence on the dip angle of the seismic source. For vertical (90°) and horizontal (0°) dip-slip double couples, the deformation field remains continuous across a welded interface, whereas for intermediate dip angles the deformation may exhibit a jump as the source crosses the interface. For two-dimensional line sources, Singh and Garg (1986) provided a compact representation of seismic sources. Rani et al. (1991) obtained expressions for displacements and stresses at arbitrary points in a uniform half-space, and Singh et al. (1992) extended these results to two welded half-spaces. Rani and Singh (1992) subsequently considered the deformation produced by a long dip-slip fault. Most of the earlier studies assume that the interface between the two media is perfectly bonded, or welded. Under this assumption, both the displacements and the tractions remain continuous across the interface. But natural contacts such as the crust–mantle (Moho) boundary,

International Research Journal on Advanced Engineering and Management
https://goldncloudpublications.com
https://doi.org/10.47392/IRJAEM.2026.0390
e ISSN: 2584-2854
Volume: 04 Issue: 08
August 2026
Page No: 2741 - 2754

sediment–basement contacts, and fault-gouge zones can contain cracks, weak bonding, or zones of relative slip. In such situations, the displacement field may not remain continuous even though the tractions are transmitted across the interface. To account for this behaviour, Yu (1998) introduced a dislocation-like model for imperfect interfaces. Fan and Wang (2003) investigated the interaction of a screw dislocation with a spring-type imperfect interface, while Ben-Zion (1990) considered dislocation sources located at material interfaces. Chu et al. (2012) studied elastic fields associated with dislocation loops near bimaterial interfaces. Wu et al. (2017) later formulated two complementary interface models: the dislocation-like interface, in which tractions remain continuous while displacements may be discontinuous, and the force-like interface, in which displacements remain continuous while tractions may undergo a discontinuity. These models provide a useful framework for describing imperfect bonding and its influence on elastic deformation. Building on this approach, Kumari and Madan (2021a) derived the deformation field produced by two-dimensional seismic sources across a dislocation-like interface and considered the special case of a vertical dip-slip fault. Kumari and Madan (2021b) investigated vertical dip-slip and tensile faults using a force-like imperfect interface, while Madan and Kumari (2022) examined the deformation caused by a vertical tensile fault. More recently, Kumari and Madan (2024) considered a strike-slip dislocation in two imperfectly coupled orthotropic elastic half-spaces. Despite these developments, the available analytical results for imperfectly bonded interfaces have been directed mainly toward vertical (90°) fault geometries. This leaves an important gap because the behaviour of an obliquely dipping source can be substantially different. In particular, the results of Heaton and Heaton (1989) indicate that intermediate dip angles can produce distinctive changes in the deformation pattern across an interface. Thus, extending imperfect-interface formulations to oblique fault geometries is important for obtaining a more complete understanding of seismic deformation. In the present study, we consider a two-dimensional dip-slip fault dipping at 45° in two homogeneous, isotropic elastic half-spaces separated by a dislocation-like imperfect interface. Following the formulation of Singh et al. (1992) and adopting the dislocation-like interface model of Wu et al. (2017), closed-form analytical expressions are derived for the Airy stress function, displacements, and stresses produced by a two-dimensional line source. The particular case of a dip-slip fault dipping at 45° is then obtained in dimensionless form. The influence of the interface bonding parameters on the resulting deformation field is investigated in detail. The perfect (welded) and traction-free (sliding) interfaces are recovered as limiting cases of the bonding matrix. The variations of dimensionless displacements and stresses are examined using line plots, displacement-discontinuity plots, and three-dimensional mesh-grid representations with contour lines.

2. Basic theory

Two homogeneous, isotropic elastic half-spaces having an imperfect interface at z = 0 are considered[1 – 10]. Cartesian coordinates are denoted by (x, y, z), and the z-axis is taken vertically downward as shown in Figure 1. A two-dimensional (yz-plane) plane-strain problem has been discussed in which displacements $u1 = 0$, $u2$ and $u3$ depend on y and z only. Medium-I is the upper half-space ($z < 0$) and medium-II is the lower half-space ($z > 0$); let $\lambda 1$, $\mu 1$ and $\lambda 2$, $\mu 2$ be elastic constants for medium-I and medium-II, respectively. Following the results of Singh et al. (1992) for a line source parallel to the x-axis passing through the point (0, 0, c) in medium II, the Airy stress functions for media I and II are:

$$U^{(\mathrm{I})} = \int_0^\infty \left[(L_1 + M_1 kz)\sin ky + (P_1 + Q_1 kz)\cos ky\right] k^{-1}\exp(kz)\,dk, \tag{1}$$

$$U^{(\mathrm{II})} = U_0 + \int_0^\infty \left[(L_2 + M_2 kz)\sin ky + (P_2 + Q_2 kz)\cos ky\right] k^{-1}\exp(-kz)\,dk, \tag{2}$$

$$U_0 = \int_0^\infty \left[(L_0 + M_0 k|z - c|)\sin ky + (P_0 + Q_0 k|z - c|)\cos ky\right] k^{-1}\exp(-k|z - c|)\,dk. \tag{3}$$

International Research Journal on Advanced Engineering and Management
https://goldncloudpublications.com
https://doi.org/10.47392/IRJAEM.2026.0390
e ISSN: 2584-2854
Volume: 04 Issue: 08
August 2026
Page No: 2741 - 2754

Superscripts (I) and (II) stand for medium I and II; Li, Mi, Pi, Qi, for i = 1, 2, are unknowns, and their values are to be calculated from the boundary conditions at the interface z = 0; the source coefficients L0, M0, P0, Q0, are independent of the variable k. The values of the source coefficients for different kinds of seismic sources are given by Singh and Garg (1986).

3. Formulation and solution

For two half-spaces having an imperfect interface at z = 0, the boundary conditions at the interface, given by Wu et al. (2017), are as shown in Figure 1 Two half-spaces having a dislocation-like interface with a line source in the lower half-space at (0, 0, c)

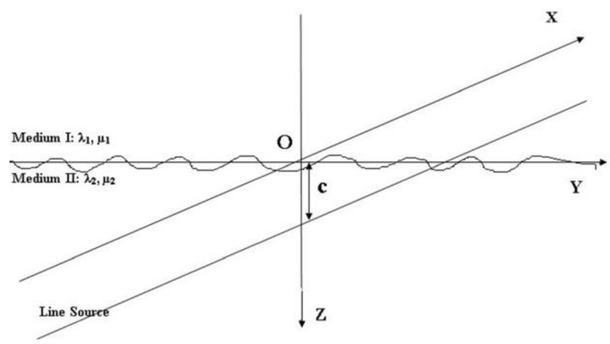

Figure 1 Two half-spaces having a dislocation-like interface with a line source in the lower half-space at (0, 0, c)

$$u_i^{(\mathrm{I})}\big|_{z^-=0} = [k_{ij}]\, u_j^{(\mathrm{II})}\big|_{z^+=0},\ i = 2, 3, \tag{4}$$

$$\tau_{i3}^{(\mathrm{I})}\big|_{z^-=0} = \tau_{i3}^{(\mathrm{II})}\big|_{z^+=0},\ i = 2, 3, \tag{5}$$

where the constant matrix $[k_{ij}]$, describes imperfect interface bonding conditions at the boundary z = 0. Let matrix $[k_{ij}]$ is assumed to be diagonal, then the first element will be related to the condition in the normal direction of the interface plane, and the last two elements on the diagonal represent interface conditions in the tangential directions. The source coefficients L_0, M_0, P_0, Q_0 have different values for z < c and z > c. Let L^-, M^-, P^-, Q^- be the values of L_0, M_0, P_0, Q_0 for z < c. Applying bonding conditions to the integral expressions for displacements and stresses derived from equations (1 and 2), we obtained:

$$\boldsymbol{E}\begin{bmatrix} L_1 \\ M_1 \\ L_2 \\ M_2 \end{bmatrix} = \begin{bmatrix} (L^- + M^- kc)\exp(-kc) \\ (L^- - M^- + M^- kc)\exp(-kc) \\ k_{22}\beta\left(L^- - \dfrac{M^-}{\alpha_2} + M^- kc\right)\exp(-kc) \\ k_{33}\beta\left(L^- - M^- + \dfrac{M^-}{\alpha_2} + M^- kc\right)\exp(-kc) \end{bmatrix}, \tag{6}$$

$$\boldsymbol{E}\begin{bmatrix} P_1 \\ Q_1 \\ P_2 \\ Q_2 \end{bmatrix} = \begin{bmatrix} (P^- + Q^- kc)\exp(-\mathrm{kc}) \\ (P^- - Q^- + Q^- kc)\exp(-\mathrm{kc}) \\ k_{22}\beta(P^- - Q^-/\alpha_2 + Q^- kc)\exp(-\mathrm{kc}) \\ k_{33}\beta(P^- - Q^- + Q^-/\alpha_2 + Q^- kc)\exp(-\mathrm{kc}) \end{bmatrix}, \tag{7}$$

Where

$$\boldsymbol{E} = \begin{bmatrix} 1 & 0 & -1 & 0 \\ 1 & 1 & 1 & -1 \\ 1 & 1/\alpha_1 & -k_{22}\beta & -k_{22}\beta/\alpha_1 \\ 1 & 1 - 1/\alpha_1 & k_{33}\beta & k_{33}\beta(1 - 1/\alpha_1) \end{bmatrix},$$

and

$$\alpha_1 = \frac{\lambda_1 + \mu_1}{\lambda_1 + 2\mu_1},\quad \alpha_2 = \frac{\lambda_2 + \mu_2}{\lambda_2 + 2\mu_2},\quad \beta = \frac{\mu_1}{\mu_2}. \tag{8}$$

On solving equations (6 and 7), we get

$$\begin{bmatrix} L_1 \\ M_1 \\ L_2 \\ M_2 \end{bmatrix} = \boldsymbol{F}\begin{bmatrix} (L^- + M^- kc)\exp(-kc) \\ M^- \exp(-kc) \end{bmatrix} \quad \text{and}$$

$$\begin{bmatrix} P_1 \\ Q_1 \\ P_2 \\ Q_2 \end{bmatrix} = \boldsymbol{F}\begin{bmatrix} (P^- + P^- kc)\exp(-kc) \\ Q^- \exp(-kc) \end{bmatrix}, \tag{9}$$

where

$$\boldsymbol{F} = \begin{bmatrix} A_1 & A_2 \\ C_1 & C_2 \\ B_1 & B_2 \\ D_1 & D_2 \end{bmatrix},$$

International Research Journal on Advanced Engineering and Management
https://goldncloudpublications.com
https://doi.org/10.47392/IRJAEM.2026.0390
e ISSN: 2584-2854
Volume: 04 Issue: 08
August 2026
Page No: 2741 - 2754

$$A_1 = (2\alpha_2\beta k_{22} + 2\alpha_2\beta k_{33} - 2\alpha_1\alpha_2\beta k_{22} + 2\alpha_1\alpha_2\beta^2 k_{22}k_{33})/D,$$

$$A_2 = (-2\alpha_2\beta k_{22} + 2\alpha_1\alpha_2\beta k_{22} + 2\alpha_1\beta^2 k_{22}k_{33} - 2\alpha_1\alpha_2\beta^2 k_{22}k_{33})/D,$$

$$B_1 = (\alpha_1{\alpha_2}^2 - 2{\alpha_2}^2 + {\alpha_2}^2\beta k_{22} + {\alpha_2}^2\beta k_{33} - \alpha_1\alpha_2\beta k_{22} + \alpha_1\alpha_2\beta k_{33} \\ - \alpha_1{\alpha_2}^2\beta k_{22} - \alpha_1{\alpha_2}^2\beta k_{33} + \alpha_1{\alpha_2}^2\beta^2 k_{22}k_{33})/D,$$

$$B_2 = (2\alpha_1\alpha_2\beta k_{22} + 2\alpha_1\beta^2 k_{22}k_{33} - 2\alpha_1\alpha_2\beta^2 k_{22}k_{33} - 2\alpha_2\beta k_{22})/D,$$

$$C_1 = (-2\alpha_1\alpha_2\beta k_{33} + 2\alpha_1\alpha_2\beta k_{22})/D,$$

$$C_2 = (-2\alpha_1\alpha_2\beta k_{22} - 4\alpha_1\beta^2 k_{22}k_{33} + 2\alpha_1\alpha_2\beta^2 k_{22}k_{33})/D,$$

$$D_1 = (-4{\alpha_2}^2 + 2\alpha_1{\alpha_2}^2 + 2{\alpha_2}^2\beta k_{22} + 2{\alpha_2}^2\beta k_{33} - 2\alpha_1{\alpha_2}^2\beta k_{22} \\ - 2\alpha_1{\alpha_2}^2\beta k_{33} + 2\alpha_1{\alpha_2}^2\beta^2 k_{22}k_{33})/D,$$

$$D_2 = (2{\alpha_2}^2 - \alpha_1{\alpha_2}^2 - 2\alpha_2\beta k_{22} + 2\alpha_2\beta k_{33} + \alpha_1\alpha_2\beta k_{22} - {\alpha_2}^2\beta k_{22} - \alpha_1\alpha_2\beta k_{33} \\ - {\alpha_2}^2\beta k_{33} + \alpha_1{\alpha_2}^2\beta k_{22} + \alpha_1{\alpha_2}^2\beta k_{33} - \alpha_1{\alpha_2}^2\beta^2 k_{22}k_{33})/D,$$

and

$$D = \alpha_2(2\alpha_2 - \alpha_1\alpha_2 + 2\beta k_{22} + 2\beta k_{33} - \alpha_1\beta k_{22} \\ - \alpha_2\beta k_{22} - \alpha_1\beta k_{33} - \alpha_2\beta k_{33} \\ + 2\alpha_1\beta^2 k_{22}k_{33} + \alpha_1\alpha_2\beta k_{22} + \alpha_1\alpha_2\beta k_{33} - \alpha_1\alpha_2\beta^2 k_{22}k_{33}).$$

Substituting values of L_1, M_1, P_1, Q_1 and L_2, M_2, P_2, Q_2 in equations (1 and 2), we get the integral expressions for Airy stress function[11 – 20], displacements and stresses; on solving these integrals, we get the results for medium-I and II as follows:

$$U^{(\mathrm{I})} = L^-\left[A_1\tan^{-1}\left(\frac{y}{c-z}\right) + C_1 z\left(\frac{y}{R^2}\right)\right] + M^-\left[A_2\tan^{-1}\left(\frac{y}{c-z}\right) + C_2 z\left(\frac{y}{R^2}\right) \\ + A_1 c\left(\frac{y}{R^2}\right) + 2C_1 czy(c-z)/R^4\right] + P^-\left[-A_1\ln R + C_1 z\left(\frac{c-z}{R^2}\right)\right] \\ + Q^-\left[-A_2\ln R + (C_2 z + A_1 c)\left(\frac{c-z}{R^2}\right) + C_1 cz\frac{1}{R^2}\left\{\frac{2(c-z)^2}{R^2} - 1\right\}\right], \quad (11)$$

$$\tau_{22}^{(\mathrm{I})} = L^-\left[2(A_1 + 2C_1)\frac{y(c-z)}{R^4} + C_1 z\frac{2y}{R^4}\left\{\frac{4(c-z)^2}{R^2} - 1\right\}\right] \\ + M^-\left[2(A_2 + 2C_2)\frac{y(c-z)}{R^4} + (A_1 c + 2C_1 c + C_2 z)\frac{2y}{R^4}\left\{\frac{4(c-z)^2}{R^2} - 1\right\} \\ + C_1 cz\frac{24y(c-z)}{R^6}\left\{\frac{2(c-z)^2}{R^2} - 1\right\}\right] + P^-\left[(A_1 + 2C_1)\frac{1}{R^2}\left\{\frac{2(c-z)^2}{R^2} - 1\right\} \\ + C_1 z\frac{2(c-z)}{R^4}\left\{\frac{4(c-z)^2}{R^2} - 3\right\}\right] + Q^-\left[(A_2 + 2C_2)\frac{1}{R^2}\left\{\frac{2(c-z)^2}{R^2} - 1\right\} \\ + (A_1 c + 2C_1 c + C_2 z)\frac{2(c-z)}{R^4}\left\{\frac{4(c-z)^2}{R^2} - 3\right\} + \\ + C_1 cz\frac{6}{R^4}\left\{\frac{8(c-z)^4}{R^4} - \frac{8(c-z)^2}{R^2} + 1\right\}\right], \quad (12)$$

$$\tau_{23}^{(\mathrm{I})} = L^-\left[-(A_1 + C_1)\frac{1}{R^2}\left\{\frac{2(c-z)^2}{R^2} - 1\right\} - C_1 z\frac{2(c-z)}{R^4}\left\{\frac{4(c-z)^2}{R^2} - 3\right\}\right] \\ + M^-\left[-(A_2 + C_2)\frac{1}{R^2}\left\{\frac{2(c-z)^2}{R^2} - 1\right\} - (A_1 c + C_1 c + C_2 z)\frac{2(c-z)}{R^4} \\ \left\{\frac{4(c-z)^2}{R^2} - 3\right\} - C_1 cz\frac{6}{R^4}\left\{\frac{8(c-z)^4}{R^4} - \frac{8(c-z)^2}{R^2} + 1\right\}\right] \\ + P^-\left[2(A_1 + C_1)\frac{y(c-z)}{R^4} + C_1 z\frac{2y}{R^4}\left\{\frac{4(c-z)^2}{R^2} - 1\right\}\right] \\ + Q^-\left[2(A_2 + C_2)\frac{y(c-z)}{R^4} + (A_1 c + C_1 c + C_2 z)\frac{2y}{R^4}\left\{\frac{4(c-z)^2}{R^2} - 1\right\} \\ + C_1 cz\frac{24y(c-z)}{R^6}\left\{\frac{2(c-z)^2}{R^2} - 1\right\}\right], \quad (13)$$

$$\tau_{33}^{(I)} = L^-\left[-2A_1\frac{y(c-z)}{R^4} - C_1 z\frac{2y}{R^4}\left\{\frac{4(c-z)^2}{R^2} - 1\right\}\right] \\ + M^-\left[-2A_2\frac{y(c-z)}{R^4} - (A_1 c + C_2 z)\frac{2y}{R^4}\left\{\frac{4(c-z)^2}{R^2} - 1\right\} \\ - C_1 cz\frac{24y(c-z)}{R^6}\left\{\frac{2(c-z)^2}{R^2} - 1\right\}\right] \\ + P^-\left[-A_1\frac{1}{R^2}\left\{\frac{2(c-z)^2}{R^2} - 1\right\} - C_1 z\frac{2(c-z)}{R^4}\left\{\frac{4(c-z)^2}{R^2} - 3\right\}\right] \\ + Q^-\left[-A_2\frac{1}{R^2}\left\{\frac{2(c-z)^2}{R^2} - 1\right\} - (A_1 c + C_2 z)\frac{2(c-z)}{R^4} \\ \left\{\frac{4(c-z)^2}{R^2} - 3\right\} - C_1 cz\frac{6}{R^4}\left\{\frac{8(c-z)^4}{R^4} - \frac{8(c-z)^2}{R^2} + 1\right\} \quad (14)$$

$$2\mu_1 u_2^{(\mathrm{I})} = L^-\left[-\left(A_1 + \frac{C_1}{\alpha_1}\right)\frac{(c-z)}{R^2} - C_1 z\frac{1}{R^2}\left\{\frac{2(c-z)^2}{R^2} - 1\right\}\right] \\ + M^-\left[-\left(A_2 + \frac{C_2}{\alpha_1}\right)\frac{(c-z)}{R^2} - \left(A_1 c + \frac{cC_1}{\alpha_1} + C_2 z\right) \\ \frac{1}{R^2}\left\{\frac{2(c-z)^2}{R^2} - 1\right\} - C_1 cz\frac{2(c-z)}{R^4}\left\{\frac{4(c-z)^2}{R^2} - 3\right\}\right] \\ + P^-\left[\left(A_1 + \frac{C_1}{\alpha_1}\frac{y}{R^2}\right) + 2C_1 z\frac{y(c-z)}{R^4}\right] \\ + Q^-\left[\left(A_2 + \frac{C_2}{\alpha_1}\right)\frac{y}{R^2} + 2\left(A_1 c + \frac{cC_1}{\alpha_1} + C_2 z\right)\right. \\ \left.\frac{y(c-z)}{R^4} + + cC_1 z\frac{2y}{R^4}\left\{\frac{4(c-z)^2}{R^2} - 1\right\}\right. \quad (15)$$

$$2\mu_1 u_3^{(1)} = L^-\left[-\left(A_1 + C_1 - \frac{C_1}{\alpha_1}\right)\frac{y}{R^2} - 2C_1 z\frac{y(c-z)}{R^4}\right] \\ + M^-\left[-\left(A_2 + C_2 - \frac{C_2}{\alpha_1}\right)\frac{y}{R^2} - 2\left(A_1 c + C_1 c - \frac{cC_1}{\alpha_1} + C_2 z\right)\right.$$

International Research Journal on Advanced Engineering and Management
https://goldncloudpublications.com
https://doi.org/10.47392/IRJAEM.2026.0390
e ISSN: 2584-2854
Volume: 04 Issue: 08
August 2026
Page No: 2741 - 2754

$$\frac{y(c-z)}{R^4} - C_1 cz\frac{2y}{R^4}\Big\{\frac{4(c-z)^2}{R^2}-1\Big\}\Big]\Big]$$

$$+P^-\Big[-\Big(A_1+C_1-\frac{C_1}{\alpha_1}\Big)\frac{(c-z)}{R^2} - C_1 z\frac{1}{R^2}\Big\{\frac{2(c-z)^2}{R^2}-1\Big\}\Big]$$

$$+Q^-\Big[-\Big(A_2+C_2-\frac{C_2}{\alpha_1}\Big)\frac{(c-z)}{R^2}$$

$$+Q^-\Big[-\Big(A_2+C_2-\frac{C_2}{\alpha_1}\Big)\frac{(c-z)}{R^2} \quad (16)$$

$$U^{(\mathrm{II})} = L_0\tan^{-1}\Big(\frac{y}{|z-c|}\Big) + M_0|z-c|\frac{y}{R^2} - P_0\ln R + Q_0\frac{(z-c)^2}{R^2}$$

$$+L^-\Big[B_1\tan^{-1}\Big(\frac{y}{z+c}\Big) + D_1 z\frac{y}{S^2}\Big]$$

$$+M^-\Big[B_2\tan^{-1}\Big(\frac{y}{z+c}\Big) + (D_2 z + B_1 c)\frac{y}{S^2} + 2D_1 cz\frac{y(z+c)}{S^4}\Big]$$

$$+P^-\Big[-B_1\ln S + D_1\frac{(z+c)}{S^2}\Big] + Q^-\Big[-B_2\ln S + (D_2 z + B_1 c)$$

$$+Q^-\Big[-B_2\ln S + (D_2 z + B_1 c) \quad (7)$$

$$\tau_{22}^{(\mathrm{II})} = 2L_0|z-c|\frac{y}{R^4} + M_0\Big[-4|z-c|\frac{y}{R^4} + |z-c|\frac{2y}{R^4}\Big\{\frac{4(z-c)^2}{R^2}-1\Big\}\Big]$$

$$+P_0\frac{1}{R^2}\Big\{\frac{2(z-c)^2}{R^2}-1\Big\}$$

$$+Q_0\Big[-2\frac{1}{R^2}\Big\{\frac{2(z-c)^2}{R^2}-1\Big\} + \frac{2(z-c)^2}{R^4}\Big\{\frac{4(z-c)^2}{R^2}-3\Big\}\Big]$$

$$+L^-\Big[2(B_1-2D_1)\frac{y(z+c)}{S^4} + D_1 z\frac{2y}{S^4}\Big\{\frac{4(z+c)^2}{S^2}-1\Big\}\Big]$$

$$+M^-\Big[2(B_2-2D_2)\frac{y(z+c)}{S^4} + (B_1 c - 2D_1 c + D_2 z)\frac{2y}{S^4}\Big\{\frac{4(z+c)^2}{S^2}-1\Big\}$$

$$+D_1 cz\frac{24y(z+c)}{S^6}\Big\{\frac{2(z+c)^2}{S^2}-1\Big\}\Big] + P^-\Big[(B_1-2D_1)\frac{1}{S^2}\Big\{\frac{2(z+c)^2}{S^2}-1\Big\}$$

$$+D_1 z\frac{2(z+c)}{S^4}\Big\{\frac{4(z+c)^2}{S^2}-3\Big\}\Big]\Big] + Q^-\Big[(B_2-2D_2)\frac{1}{S^2}\Big\{\frac{2(z+c)^2}{S^2}-1\Big\}$$

$$+(B_1 c - 2D_1 c + D_2 z)\frac{2(z+c)}{S^4}\Big\{\frac{4(z+c)^2}{S^2}-3\Big\}$$

$$+D_1 cz\frac{6}{S^4}\Big\{\frac{8(z+c)^4}{S^4} - \frac{8(z+c)^2}{S^2}+1\Big\}\Big]\Big], \quad (18)$$

$$\tau_{23}^{(\mathrm{II})} = \pm\Big[L_0\frac{1}{R^2}\Big\{\frac{2(z-c)^2}{R^2}-1\Big\} - M_0\Big\{\frac{1}{R^2}\Big\{\frac{2(z-c)^2}{R^2}-1\Big\} - \frac{2(z-c)^2}{R^4}\Big\{\frac{4(z-c)^2}{R^2}-3\Big\}\Big\}\Big]$$

$$-P_0 2|z-c|\frac{y}{R^4} + Q_0\Big\{2|z-c|\frac{y}{R^4} - |z-c|\frac{2y}{R^4}\Big\{\frac{4(z-c)^2}{R^2}-1\Big\}\Big\}\Big] + L^-\Big[(B_1-D_1)\frac{1}{S^2}\Big\{\frac{2(z+c)^2}{S^2}-1\Big\}$$

$$+D_1 z\frac{2(z+c)}{S^4}\Big\{\frac{4(z+c)^2}{S^2}-3\Big\}\Big]\Big]$$

$$+M^-\Big[(B_2-D_2)\frac{1}{S^2}\Big\{\frac{2(z+c)^2}{S^2}-1\Big\}$$

$$+(B_1 c - D_1 c + D_2 z)\frac{2(z+c)}{S^4}\Big\{\frac{4(z+c)^2}{S^2}-3\Big\}$$

$$+D_1 cz\frac{6}{S^4}\Big\{\frac{8(z+c)^4}{S^4} - \frac{8(z+c)^2}{S^2}+1\Big\}\Big]\Big]$$

$$+P^-\Big[-2(B_1-D_1)\frac{y(z+c)}{S^4}$$

$$-D_1 z\frac{2y}{S^4}\Big\{\frac{4(z+c)^2}{S^2}-1\Big\}\Big]\Big]$$

$$+Q^-\Big[-2(B_2-D_2)\frac{y(z+c)}{S^4} - (B_1 c - D_1 c + D_2 z)\frac{2y}{S^4}$$

$$\Big\{\frac{4(z+c)^2}{S^2}-1\Big\}$$

$$-D_1 cz\frac{24y(z+c)}{S^6}\Big\{\frac{2(z+c)^2}{S^2}-1\Big\}\Big]\Big], \quad (19)$$

$$\tau_{33}^{(\mathrm{II})} = -L_0 2|z-c|\frac{y}{R^4} - M_0|z-c|\frac{2y}{R^4}\Big\{\frac{4(z-c)^2}{R^2}-1\Big\} - P_0\frac{1}{R^2}\Big\{\frac{2(z-c)^2}{R^2}-1\Big\}$$

$$-Q_0\frac{2(z-c)^2}{R^4}\Big\{\frac{4(z-c)^2}{R^2}-3\Big\} + L^-\Big[-2B_1\frac{y(z+c)}{S^4}$$

$$-D_1 z\frac{2y}{S^4}\Big\{\frac{4(z+c)^2}{S^2}-1\Big\}\Big]\Big]$$

$$+M^-\Big[-2B_2\frac{y(z+c)}{S^4} - (B_1 c + D_2 z)\frac{2y}{S^4}\Big\{\frac{4(z+c)^2}{S^2}-1\Big\}$$

$$-D_1 cz\frac{24y(z+c)}{S^6}\Big\{\frac{2(z+c)^2}{S^2}-1\Big\}\Big]\Big]$$

$$+P^-\Big[-B_1\frac{1}{S^2}\Big\{\frac{2(z+c)^2}{S^2}-1\Big\} - D_1 z\frac{2(z+c)}{S^4}\Big\{\frac{4(z+c)^2}{S^2}-3\Big\}\Big]$$

$$+Q^-\Big[-B_2\frac{1}{S^2}\Big\{\frac{2(z+c)^2}{S^2}-1\Big\} - (B_1 c + D_2 z)\frac{2(z+c)}{S^4}\Big\{\frac{4(z+c)^2}{S^2}-3\Big\}$$

$$-D_1 cz\frac{6}{S^4}\Big\{\frac{8(z+c)^4}{S^4} - \frac{8(z+c)^2}{S^2}+1\Big\}\Big]$$

$$2\mu_2 u_2^{(\mathrm{II})} = -L_0\frac{|z-c|}{R^2} + M_0\Big[\frac{|z-c|}{\alpha_2 R^2} - |z-c|\frac{1}{R^2}\Big\{\frac{2(z-c)^2}{R^2}-1\Big\}\Big]$$

$$+P_0\frac{y}{R^2} - Q_0\Big[\frac{y}{\alpha_2 R^2} - 2(z-c)^2\frac{y}{R^4}\Big]$$

$$+L^-\Big[(-B_1 + D_1/\alpha_2)\frac{(z+c)}{S^2} - D_1 z\frac{1}{S^2}\Big\{\frac{2(z+c)^2}{S^2}-1\Big\}\Big]$$

$$+M^-\Big[(-B_2 + D_2/\alpha_2)\frac{(z+c)}{S^2} + \Big(-B_1 c + \frac{cD_1}{\alpha_2} - D_2 z\Big)$$

International Research Journal on Advanced Engineering and Management
https://goldncloudpublications.com
https://doi.org/10.47392/IRJAEM.2026.0390
e ISSN: 2584-2854
Volume: 04 Issue: 08
August 2026
Page No: 2741 - 2754

$$\frac{1}{S^2}\left\{\frac{2(z+c)^2}{S^2}-1\right\}-D_1 cz\frac{2(z+c)}{S^4}\left\{\frac{4(z+c)^2}{S^2}-3\right\}\Bigg]$$

$$+P^-\left[(B_1-D_1/\alpha_2)\frac{y}{S^2}+D_1 z\frac{2y(z+c)}{S^4}\right]$$

$$+Q^-\Bigg[\left(B_2-\frac{D_2}{\alpha_2}\right)\frac{y}{S^2}+\left(B_1 c-\frac{cD_1}{\alpha_2}+D_2 z\right)$$

$$\frac{2y(z+c)}{S^4}+D_1 cz\frac{2y}{S^4}\left\{\frac{4(z+c)^2}{S^2}-1\right\}\Bigg] \quad (21)$$

$$2\mu_2 u_3^{(\mathrm{II})}=\pm\Bigg[L_0\frac{y}{R^2}-M_0\left\{\frac{y}{R^2}-\frac{y}{\alpha_2 R^2}-2(z-c)^2\frac{y}{R^4}\right\}+P_0\frac{|z-c|}{R^2}$$

$$-Q_0\left\{\frac{|z-c|}{R^2}-\frac{|z-c|}{\alpha_2 R^2}-|z-c|\frac{1}{R^2}\left\{\frac{2(z-c)^2}{R^2}-1\right\}\right\}\Bigg]$$

$$+L^-\left[(B_1-D_1+D_1/\alpha_2)\frac{y}{S^2}+D_1 z\frac{2y(z+c)}{S^4}\right]$$

$$+M^-\Bigg[(B_2-D_2+D_2/\alpha_2)\frac{y}{S^2}+\left(B_1 c-cD_1+\frac{cD_1}{\alpha_2}+D_2 z\right)$$

$$\frac{2y(z+c)}{S^4}+D_1 cz\frac{2y}{S^4}\left\{\frac{4(z+c)^2}{S^2}-1\right\}$$

$$P^-\left[(B_1-D_1+D_1/\alpha_2)\frac{(z+c)}{S^2}+D_1 z\frac{1}{S^2}\left\{\frac{2(z+c)^2}{S^2}-1\right\}\right]$$

$$+Q^-\Bigg[(B_2-D_2+D_2/\alpha_2)\frac{(z+c)}{S^2}+\left(B_1 c-cD_1+\frac{cD_1}{\alpha_2}+D_2 z\right)$$

$$\frac{1}{S^2}\left\{\frac{2(z+c)^2}{S^2}-1\right\}+D_1 cz\frac{2(z+c)}{S^4}\left\{\frac{4(z+c)^2}{S^2}-3\right\}\Bigg] \quad (22)$$

$$2\mu_1 u_2^{(\mathrm{I})}=L^-\left[-A_1\frac{(c-z)}{R^2}\right]+M^-\left[-\left(A_2+\frac{C_2}{\alpha_1}\right)\frac{(c-z)}{R^2}-(A_1 c+C_2 z)\right.$$

$$2\mu_1 u_2^{(\mathrm{I})}=L^-\left[-A_1\frac{(c-z)}{R^2}\right]+M^-\left[-\left(A_2+\frac{C_2}{\alpha_1}\right)\frac{(c-z)}{R^2}-(A_1 c+C_2 z)\right.$$

where $R^2 = y^2 + (z-c)^2$ and $S^2 = y^2 + (z+c)^2$.

3.1. Perfect (welded) interface case

3.1.1. Medium-I

On substituting $k_{22} = k_{33} = 1$, the interface becomes perfect, and the corresponding expressions for Airy stress function, displacements and stresses in medium-I are as follows:

$$U^{(\mathrm{I})}=L^-\left[A_1\tan^{-1}\left(\frac{y}{c-z}\right)\right]+M^-\left[A_2\tan^{-1}\left(\frac{y}{c-z}\right)\right.$$

$$\left.+(C_2 z+A_1 c)\frac{y}{R^2}\right]+P^-[-A_1\ln R]$$

$$+Q^-\left[-A_2\ln R+(C_2 z+A_1 c)\left(\frac{c-z}{R^2}\right)\right], \quad (23)$$

$$\tau_{22}^{(\mathrm{I})}=L^-\left[2A_1\frac{y(c-z)}{R^4}\right]+M^-\Bigg[2(A_2+2C_2)\frac{y(c-z)}{R^4}$$

$$+(A_1 c+C_2 z)\frac{2y}{R^4}\left\{\frac{4(c-z)^2}{R^2}-1\right\}\Bigg]$$

$$+P^-\left[A_1\frac{1}{R^2}\left\{\frac{2(c-z)^2}{R^2}-1\right\}\right]+Q^-\Bigg[(A_2+2C_2)\cdot$$

$$\frac{2y}{R^4}\left\{\frac{4(c-z)^2}{R^2}-1\right\}\Bigg]$$

$$+(A_1 c+C_2 z)\frac{2(c-z)}{R^4}\left\{\frac{4(c-z)^2}{R^2}-3\right\}\Bigg], \quad (24)$$

$$\tau_{23}^{(\mathrm{I})}=L^-\left[-A_1\frac{1}{R^2}\left\{\frac{2(c-z)^2}{R^2}-1\right\}\right]+M^-\Bigg[-(A_2+C_2)\frac{1}{R^2}\left\{\frac{2(c-z)^2}{R^2}-1\right\}$$

$$-(A_1 c+C_2 z)\frac{2(c-z)}{R^4}\left\{\frac{4(c-z)^2}{R^2}-3\right\}\Bigg]+P^-\left[2A_1\frac{y(c-z)}{R^4}\right]$$

$$+Q^-\left[2(A_2+C_2)\frac{y(c-z)}{R^4}+(A_1 c+C_2 z)\frac{2y}{R^4}\left\{\frac{4(c-z)^2}{R^2}-1\right\}\right], \quad (25)$$

$$\tau_{33}^{(\mathrm{I})}=L^-\left[-2A_1\frac{y(c-z)}{R^4}\right]+M^-\left[-2A_2\frac{y(c-z)}{R^4}-(A_1 c+C_2 z)\frac{2y}{R^4}\left\{\frac{4(c-z)^2}{R^2}-1\right\}\right]$$

$$+P^-\left[-A_1\frac{1}{R^2}\left\{\frac{2(c-z)^2}{R^2}-1\right\}\right]+Q^-\Bigg[-A_2\frac{1}{R^2}\left\{\frac{2(c-z)^2}{R^2}-1\right\}$$

$$-(A_1 c+C_2 z)\frac{2(c-z)}{R^4}\left\{\frac{4(c-z)^2}{R^2}-3\right\}\Bigg], \quad (26)$$

$$2\mu_1 u_2^{(\mathrm{I})}=L^-\left[-A_1\frac{(c-z)}{R^2}\right]+M^-\Bigg[-\left(A_2+\frac{C_2}{\alpha_1}\right)\frac{(c-z)}{R^2}-(A_1 c+C_2 z)$$

$$\frac{1}{R^2}\left\{\frac{2(c-z)^2}{R^2}-1\right\}\Bigg]+P^-\left[A_1\frac{y}{R^2}\right]$$

$$+Q^-\left[\left(A_2+\frac{C_2}{\alpha_1}\right)\frac{y}{R^2}+2(A_1 c+C_2 z)\frac{y(c-z)}{R^4}\right], \quad (27)$$

$$2\mu_1 u_3^{(\mathrm{I})}=L^-\left[-A_1\frac{y}{R^2}\right]+M^-\Bigg[\left(-A_2+C_2-\frac{C_2}{\alpha_1}\right)\frac{y}{R^2}$$

$$-2(A_1 c+C_2 z)\frac{y(c-z)}{R^4}\Bigg]+P^-\left[-A_1\frac{(c-z)}{R^2}\right]$$

$$+Q^-\Bigg[-(A_2+C_2-\frac{C_2}{\alpha_1})\frac{(c-z)}{R^2}-(A_1 c+C_2 z)$$

International Research Journal on Advanced Engineering and Management
https://goldncloudpublications.com
https://doi.org/10.47392/IRJAEM.2026.0390
e ISSN: 2584-2854
Volume: 04 Issue: 08
August 2026
Page No: 2741 - 2754

$$\left.\frac{1}{R^2}\left\{\frac{2(c-z)^2}{R^2}-1\right\}\right], \quad (28)$$

where

$$A_1 = (4\alpha_2\beta - 2\alpha_1\alpha_2\beta + 2\alpha_1\alpha_2\beta^2)/D,$$
$$A_2 = (-2\alpha_2\beta + 2\alpha_1\alpha_2\beta + 2\alpha_1\beta^2 - 2\alpha_1\alpha_2\beta^2)/D,$$
$$C_2 = (-2\alpha_1\alpha_2\beta - 4\alpha_1\beta^2 + 2\alpha_1\alpha_2\beta^2)/D, \quad (29)$$

and

$$D = \alpha_2\big(2\alpha_2 - \alpha_1\alpha_2 + 4\beta - 2\alpha_1\beta - 2\alpha_2\beta + 2\alpha_1\beta^2 + 2\alpha_1\alpha_2\beta - \alpha_1\alpha_2\beta^2\big). \quad (30)$$

3.1.2. Medium-II

For medium-II, when the interface is perfect, the corresponding expressions for Airy's stress function, displacements and stresses are equations (17–22) with the reduced coefficients as follows (after taking $k_{22} = k_{33} = 1$);

$$B_1 = (\alpha_1\alpha_2{}^2 - 2\alpha_2{}^2 + 2\alpha_2{}^2\beta - 2\alpha_1\alpha_2{}^2\beta + \alpha_1\alpha_2{}^2\beta^2)/D,$$
$$B_2 = (2\alpha_1\alpha_2\beta + 2\alpha_1\beta^2 - 2\alpha_1\alpha_2\beta^2 - 2\alpha_2\beta)/D,$$
$$D_1 = D_3 = (-4\alpha_2{}^2 + 2\alpha_1\alpha_2{}^2 + 4\alpha_2{}^2\beta - 4\alpha_1\alpha_2{}^2\beta + 2\alpha_1\alpha_2{}^2\beta^2)/D,$$
$$D_2 = (2\alpha_2{}^2 - \alpha_1\alpha_2{}^2 - 2\alpha_2{}^2\beta + 2\alpha_1\alpha_2{}^2\beta - \alpha_1\alpha_2{}^2\beta^2)/D, \quad (31)$$

and D is obtained above in equation (30). Results obtained above equations (23–31) with a perfect bonding interface for medium-I and II coincide with the corresponding results already obtained by Singh *et al.* (1992).

3.2.Rigid interface case

If we substitute $k_{22} = k_{33} = 0$, the corresponding displacements and stresses for two isotropic elastic half-spaces having a rigid interface can be obtained.

4. Dip–slip fault at 45° case

A fault is defined as a plane fracture between two blocks, and a dip is defined as the angle of the fault with respect to the surface. A dip–slip fault at 450 occurred due to a double-couple (23)+(32) mechanism of seismic sources, which allows relative movement of blocks vertically and the moment of the double couple D23 is given by Singh et al. (1992) as follows[21 – 27]:

$$D_{23} = \mu_2 bds, \quad (32)$$

where b is slip, ds is the width of the line source, and μ2 is the rigidity of medium-II. The values of source coefficients for a dip–slip at 450 are given by Singh and Garg (1986), are

$$L_0 = M_0 = P_0 = 0, Q_0 = \pm\frac{\alpha D_{23}}{\pi}$$

where the upper sign is for z > c and the lower sign is for z < c and α = (λ+μ)/(λ+2μ). Therefore,

The source coefficient values are:

$$L_0 = M_0 = P_0 = 0, \quad Q_0 = \frac{\alpha_2\mu_2 bds}{\pi};$$
$$L^- = M^- = P^- = 0, \quad Q^- = -\frac{\alpha_2\mu_2 bds}{\pi}. \quad (33)$$

Substituting these values in equations (11–22), results for displacements and stresses for medium-I and II are obtained as

$$U^{(\mathrm{I})} = -\frac{\alpha_2\mu_2 bds}{\pi}\Big[-A_2\ln R + (C_2z + A_1c)\frac{(c-z)}{R^2} + C_1cz\frac{1}{R^2}\Big\{\frac{2(c-z)^2}{R^2}-1\Big\}\Big] \quad (34)$$

$$\tau_{22}^{(\mathrm{I})} = -\frac{\alpha_2\mu_2 bds}{\pi}\Big[(A_2+2C_2)\frac{1}{R^2}\Big\{\frac{2(c-z)^2}{R^2}-1\Big\} + (A_1c+2C_1c+C_2z)\frac{2(c-z)}{R^4}\Big\{\frac{4(c-z)^2}{R^2}-3\Big\} + C_1cz\frac{6}{R^4}\Big\{\frac{8(c-z)^4}{R^4}-\frac{8(c-z)^2}{R^2}+1\Big\}\Big] \quad (35)$$

$$\tau_{23}^{(\mathrm{I})} = -\frac{\alpha_2\mu_2 bds}{\pi}\Big[2(A_2+C_2)\frac{y(c-z)}{R^4} + (A_1c+C_1c+C_2z)\frac{2y}{R^4}\Big\{\frac{4(c-z)^2}{R^2}-1\Big\} + C_1cz\frac{24y(c-z)}{R^6}\Big\{\frac{2(c-z)^2}{R^2}-1\Big\}\Big] \quad (36)$$

$$\tau_{33}^{(\mathrm{I})} = -\frac{\alpha_2\mu_2 bds}{\pi}\Big[-A_2\frac{1}{R^2}\Big\{\frac{2(c-z)^2}{R^2}-1\Big\} - (A_1c+C_2z)\frac{2(c-z)}{R^4}\Big\{\frac{4(c-z)^2}{R^2}-3\Big\} - C_1cz\frac{6}{R^4}\Big\{\frac{8(c-z)^4}{R^4}-\frac{8(c-z)^2}{R^2}+1\Big\}\Big] \quad (37)$$

$$2\mu_1u_2^{(\mathrm{I})} = -\frac{\alpha_2\mu_2 bds}{\pi}\Big[\Big(A_2+\frac{C_2}{\alpha_1}\Big)\frac{y}{R^2} + 2\Big(A_1c+\frac{cC_1}{\alpha_1}+C_2z\Big)\frac{y(c-z)}{R^4} + C_1cz\frac{2y}{R^4}\Big\{\frac{4(c-z)^2}{R^2}-1\Big\}\Big] \quad (38)$$

International Research Journal on Advanced Engineering and Management
https://goldncloudpublications.com
https://doi.org/10.47392/IRJAEM.2026.0390
e ISSN: 2584-2854
Volume: 04 Issue: 08
August 2026
Page No: 2741 - 2754

$$
\begin{aligned}
2\mu_1 u_3^{(\mathrm{I})} = -\frac{\alpha_2\mu_2 bds}{\pi}\Big[&-\Big(A_2 + C_2 - \frac{C_2}{\alpha_1}\Big)\frac{(c-z)}{R^2} \\
&- \Big(A_1 c + C_1 c - \frac{cC_1}{\alpha_1} + C_2 z\Big)\frac{1}{R^2}\Big\{\frac{2(c-z)^2}{R^2} - 1\Big\} \\
&- C_1 cz\,\frac{2(c-z)}{R^4}\Big\{\frac{4(c-z)^2}{R^2} - 3\Big\}\Big]
\end{aligned} \tag{39}
$$

$$
\begin{aligned}
U^{(\mathrm{II})} = \frac{\alpha_2\mu_2 bds}{\pi}\Big[&\frac{(z-c)^2}{R^2} + B_2 \ln S - (D_2 z + B_1 c)\frac{(z+c)}{S^2} \\
&- D_1 cz\,\frac{1}{S^2}\Big\{\frac{2(z+c)^2}{S^2} - 1\Big\}\Big]
\end{aligned} \tag{40}
$$

$$
\begin{aligned}
\tau_{22}^{(\mathrm{II})} = \frac{\alpha_2\mu_2 bds}{\pi}\Big[&-\frac{2}{R^2}\Big\{\frac{2(z-c)^2}{R^2} - 1\Big\} + \frac{2(z-c)^2}{R^4}\Big\{\frac{4(z-c)^2}{R^2} - 3\Big\} \\
&- (B_2 - 2D_2)\frac{1}{S^2}\Big\{\frac{2(z+c)^2}{S^2} - 1\Big\} \\
&- (B_1 c - 2D_1 c + D_2 z)\frac{2(z+c)}{S^4}\Big\{\frac{4(z+c)^2}{S^2} - 3\Big\} \\
&- D_1 cz\,\frac{6}{S^4}\Big\{\frac{8(z+c)^4}{S^4} - \frac{8(z+c)^2}{S^2} + 1\Big\}\Big]
\end{aligned} \tag{41}
$$

$$
\begin{aligned}
\tau_{33}^{(\mathrm{II})} = \frac{\alpha_2\mu_2 bds}{\pi}\Big[&-\frac{2(z-c)^2}{R^4}\Big\{\frac{4(z-c)^2}{R^2} - 3\Big\} + B_2\frac{1}{S^2}\Big\{\frac{2(z+c)^2}{S^2} - 1\Big\} \\
&+ (B_1 c + D_2 z)\frac{2(z+c)}{S^4}\Big\{\frac{4(z+c)^2}{S^2} - 3\Big\} \\
&+ D_1 cz\,\frac{6}{S^4}\Big\{\frac{8(z+c)^4}{S^4} - \frac{8(z+c)^2}{S^2} + 1\Big\}\Big]
\end{aligned} \tag{42}
$$

$$
\begin{aligned}
\tau_{23}^{(\mathrm{II})} = \frac{\alpha_2\mu_2 bds}{\pi}\Big[&\frac{2(z-c)y}{R^4} - (z-c)\frac{2y}{R^4}\Big\{\frac{4(z-c)^2}{R^2} - 1\Big\} \\
&+ 2(B_2 - D_2)\frac{y(z+c)}{S^4} + (B_1 c - D_1 c + D_2 z)\frac{2y}{S^4}\Big\{\frac{4(z+c)^2}{S^2} - 1\Big\} \\
&+ D_1 cz\,\frac{24y(z+c)}{S^6}\Big\{\frac{2(z+c)^2}{S^2} - 1\Big\}\Big]
\end{aligned} \tag{43}
$$

$$
\begin{aligned}
2\mu_2 u_2^{(\mathrm{II})} = \frac{\alpha_2\mu_2 bds}{\pi}\Big[&-\frac{y}{\alpha_2 R^2} + 2(z-c)^2\frac{y}{R^4} - (B_2 - D_2/\alpha_2)\frac{y}{S^2} \\
&- (B_1 c - cD_1/\alpha_2 + D_2 z)\frac{2y(z+c)}{S^4} \\
&- D_1 cz\,\frac{2y}{S^4}\Big\{\frac{4(z+c)^2}{S^2} - 1\Big\}\Big]
\end{aligned} \tag{44}
$$

$$
\begin{aligned}
2\mu_2 u_3^{(\mathrm{II})} = \frac{\alpha_2\mu_2 bds}{\pi}\Big[&-\frac{(z-c)}{R^2} + \frac{(z-c)}{\alpha_2 R^2} + (z-c)\frac{1}{R^2}\Big\{\frac{2(z-c)^2}{R^2} - 1\Big\} \\
&- (B_2 - D_2 + D_2/\alpha_2)\frac{(z+c)}{S^2} \\
&- \Big(B_1 c - cD_1 + \frac{cD_1}{\alpha_2} + D_2 z\Big)\frac{1}{S^2}\Big\{\frac{2(z+c)^2}{S^2} - 1\Big\} \\
&- D_1 cz\,\frac{2(z+c)}{S^4}\Big\{\frac{4(z+c)^2}{S^2} - 3\Big\}\Big]
\end{aligned} \tag{45}
$$

where $R^2 = y^2 + (z - c)^2$ and

$$S^2 = y^2 + (z + c)^2;$$

the coefficients A_1, A_2, B_1,B_2,C_1,C_2,D_1,〖and D〗_2 are as defined in equation (10).

5. Numerical results and discussion

For the numerical work, the continental–crust model is used, with $\alpha_1 = \alpha_2 = 0.685$ and $\beta = \mu_1/\mu_2 = 0.451$. Dimensionless coordinates $Y = y/c$ (distance from the fault) and $Z = z/c$ (distance from the interface) are introduced, where c is the depth of the line source below the interface. The displacements are measured in units of $bds/\pi c$ and the stresses in units of $\mu_2 bds/\pi c^2$. Let the dimensionless displacements and stresses be defined as:

$$U_i^{(I)} = \frac{\pi c u_i^{(I)}}{bds} \text{ and } U_i^{(II)} = \frac{\pi c u_i^{(II)}}{bds}$$

with $A^2 = Y^2 + (Z - 1)^2$ and $B^2 = Y^2 + (Z + 1)^2$

Therefore, the displacements obtained above in equations (38, 39, 44, 45) can be expressed in dimensionless form as:

$$
\begin{aligned}
U_2^{(\mathrm{I})} = -\frac{\alpha_2}{2\beta}\Big[&\Big(A_2 + \frac{C_2}{\alpha_1}\Big)\frac{Y}{A^2} + 2\Big(A_1 + \frac{C_1}{\alpha_1} + C_2 Z\Big)\frac{Y(1-Z)}{A^4} \\
&+ 2C_1 Z\,\frac{Y}{A^4}\Big\{\frac{4(1-Z)^2}{A^2} - 1\Big\}\Big]
\end{aligned} \tag{46}
$$

$$
\begin{aligned}
U_3^{(\mathrm{I})} = -\frac{\alpha_2}{2\beta}\Big[&-\Big(A_2 + C_2 - \frac{C_2}{\alpha_1}\Big)\frac{(1-Z)}{A^2} \\
&- \Big(A_1 + C_1 - \frac{C_1}{\alpha_1} + C_2 Z\Big)\frac{1}{A^2}\Big\{\frac{2(1-Z)^2}{A^2} - 1\Big\} \\
&- 2C_1 Z\,\frac{(1-Z)}{A^4}\Big\{\frac{4(1-Z)^2}{A^2} - 3\Big\}\Big]
\end{aligned} \tag{47}
$$

$$
\begin{aligned}
U_2^{(\mathrm{II})} = \frac{\alpha_2}{2}\Big[&-\frac{1}{\alpha_2}\frac{Y}{A^2} + 2(Z-1)^2\frac{Y}{A^4} - \Big(B_2 - \frac{D_2}{\alpha_2}\Big)\frac{Y}{B^2} \\
&- 2\Big(B_1 - \frac{D_1}{\alpha_2} + D_2 Z\Big)\frac{Y(Z+1)}{B^4} - 2D_1 Z\,\frac{Y}{B^4}\Big\{\frac{4(Z+1)^2}{B^2} - 1\Big\}\Big]
\end{aligned} \tag{48}
$$

$$
\begin{aligned}
U_3^{(\mathrm{II})} = \frac{\alpha_2}{2}\Big[&-\frac{(Z-1)}{A^2} + \frac{1}{\alpha_2}\frac{(Z-1)}{A^2} + (Z-1)\frac{1}{A^2}\Big\{\frac{2(Z-1)^2}{A^2} - 1\Big\} \\
&- \Big(B_2 - D_2 + \frac{D_2}{\alpha_2}\Big)\frac{(Z+1)}{B^2} \\
&- \Big(B_1 - D_1 + \frac{D_1}{\alpha_2} + D_2 Z\Big)\frac{1}{B^2}\Big\{\frac{2(Z+1)^2}{B^2} - 1\Big\} \\
&- 2D_1 Z\,\frac{(Z+1)}{B^4}\Big\{\frac{4(Z+1)^2}{B^2} - 3\Big\}\Big]
\end{aligned} \tag{49}
$$

where $A^2 = Y^2 + (Z - 1)^2$ and

$B^2 = Y + (Z + 1)^2$;

the coefficients A_1, A_2, $B_1, B_2, C_1, C_2, D_1, D_2$ are as defined in equation (10).

The stresses are calculated in units of $\mu_2 bds/\pi c^2$.

with $\sigma_{ij}^{(I)} = \pi c^2 \tau_{ij}^{(I)}/\mu_2 bds$

International Research Journal on Advanced Engineering and Management
https://goldncloudpublications.com
https://doi.org/10.47392/IRJAEM.2026.0390
e ISSN: 2584-2854
Volume: 04 Issue: 08
August 2026
Page No: 2741 - 2754

and $\sigma_{ij}^{(II)} = \pi c^2 \tau_{ij}^{(II)} / \mu_2 bds$,
the stresses of equations (35-37) and (41-43) reduce to the dimensionless forms given below:

$$\sigma_{22}^{(I)} = -\alpha_2\Big[(A_2 + 2C_2)\frac{1}{A^2}\left\{\frac{2(1-Z)^2}{A^2} - 1\right\} + (A_1 + 2C_1 + C_2 Z)\frac{2(1-Z)}{A^4}\left\{\frac{4(1-Z)^2}{A^2} - 3\right\} + C_1 Z\frac{6}{A^4}\left\{\frac{8(1-Z)^4}{A^4} - \frac{8(1-Z)^2}{A^2} + 1\right\}\Big] \quad (50)$$

$$\sigma_{23}^{(I)} = -\alpha_2\Big[2(A_2 + C_2)\frac{Y(1-Z)}{A^4} + (A_1 + C_1 + C_2 Z)\frac{2Y}{A^4}\left\{\frac{4(1-Z)^2}{A^2} - 1\right. + C_1 Z\frac{24Y(1-Z)}{A^6}\left\{\frac{2(1-Z)^2}{A^2} - 1\right\}\Big] \quad (51)$$

$$\sigma_{33}^{(I)} = -\alpha_2\Big[-A_2\frac{1}{A^2}\left\{\frac{2(1-Z)^2}{A^2} - 1\right\} - (A_1 + C_2 Z)\frac{2(1-Z)}{A^4}\left\{\frac{4(1-Z)^2}{A^2} - 3\right\} - C_1 Z\frac{6}{A^4}\left\{\frac{8(1-Z)^4}{A^4} - \frac{8(1-Z)^2}{A^2} + 1\right\}\Big] \quad (52)$$

$$\sigma_{22}^{(II)} = \alpha_2\Big[-\frac{2}{A^2}\left\{\frac{2(Z-1)^2}{A^2} - 1\right\} + \frac{2(Z-1)^2}{A^4}\left\{\frac{4(Z-1)^2}{A^2} - 3\right\} - (B_2 - 2D_2)\frac{1}{B^2}\left\{\frac{2(Z+1)^2}{B^2} - 1\right\} - (B_1 - 2D_1 + D_2 Z)\frac{2(Z+1)}{B^4}\left\{\frac{4(Z+1)^2}{B^2} - 3\right\} - D_1 Z\frac{6}{B^4}\left\{\frac{8(Z+1)^4}{B^4} - \frac{8(Z+1)^2}{B^2} + 1\right\}\Big] \quad (53)$$

$$\sigma_{23}^{(II)} = \alpha_2\Big[\frac{2Y(Z-1)}{A^4} - (Z-1)\frac{2Y}{A^4}\left\{\frac{4(Z-1)^2}{A^2} - 1\right\} + 2(B_2 - D_2)\frac{Y(Z+1)}{B^4} + (B_1 - D_1 + D_2 Z)\frac{2Y}{B^4}\left\{\frac{4(Z+1)^2}{B^2} - 1\right\} + D_1 Z\frac{24Y(Z+1)}{B^6}\left\{\frac{2(Z+1)^2}{B^2} - 1\right\}\Big] \quad (54)$$

$$\sigma_{33}^{(II)} = \alpha_2\Big[-\frac{2(Z-1)^2}{A^4}\left\{\frac{4(Z-1)^2}{A^2} - 3\right\} + B_2\frac{1}{B^2}\left\{\frac{2(Z+1)^2}{B^2} - 1\right\} + (B_1 + D_2 Z)\frac{2(Z+1)}{B^4}\left\{\frac{4(Z+1)^2}{B^2} - 3\right\} + D_1 Z\frac{6}{B^4}\left\{\frac{8(Z+1)^4}{B^4} - \frac{8(Z+1)^2}{B^2} + 1\right\}\Big] \quad (55)$$

where $A^2 = Y^2 + (Z-1)^2$ and
$B^2 = Y + (Z+1)^2$;
Y is the distance from the fault and Z is the distance from the interface; the coefficients A_1, A_2, $B_1, B_2, C_1, C_2, D_1, D_2$ are as defined in equation (10).

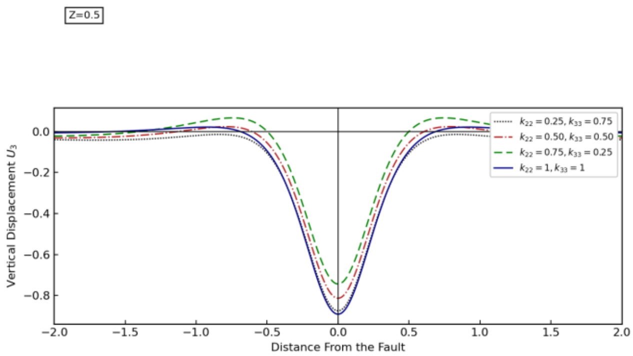

Figure 2 Variations of vertical displacement U_3 due to a perfect and an imperfect interface in medium-II

As shown in Figure 2 shows the dimensionless vertical displacement U_3 in medium–II at Z = 0.5. The response is symmetric about the fault and attains its largest (subsidence) value on the fault plane (Y = 0), the welded interface ($k_{22} = k_{33} = 1$) producing the deepest trough; imperfect bonding reduces the near–fault subsidence, while the imperfect curves decay more slowly so that their relative order reverses in the far field.

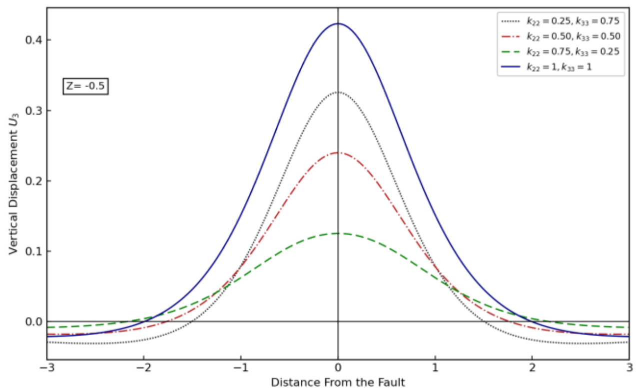

Figure 3 Variations of vertical displacement U_3 due to a perfect and an imperfect interface in medium-I

As shown in Figure 3 gives U_3 in medium–I at Z = –0.5. The response is a symmetric peak (uplift) centred on the fault whose amplitude is greatest for the perfect interface and decreases monotonically as the bonding weakens, so that imperfection systematically

International Research Journal on Advanced Engineering and Management
https://goldncloudpublications.com
https://doi.org/10.47392/IRJAEM.2026.0390
e ISSN: 2584-2854
Volume: 04 Issue: 08
August 2026
Page No: 2741 - 2754

suppresses the vertical displacement transmitted into the upper half–space. For this 45° source, U_3 is an even function of Y.

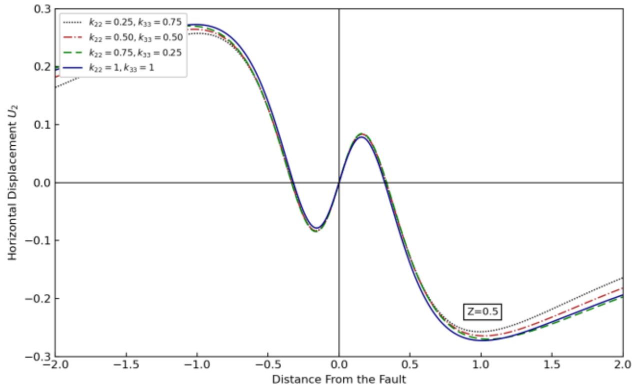

Figure 4 Variations of horizontal displacement U_2 due to a perfect and an imperfect interface in medium-II

As shown in Figure 4 depicts the horizontal displacement U_2 in medium–II at Z = 0.5. U_2 is antisymmetric about the fault, vanishing at Y = 0 and forming the characteristic S–shape with a dominant lobe near |Y| ≈ 1; close to the source, the three bonding cases almost coincide and separate mainly in the far field.

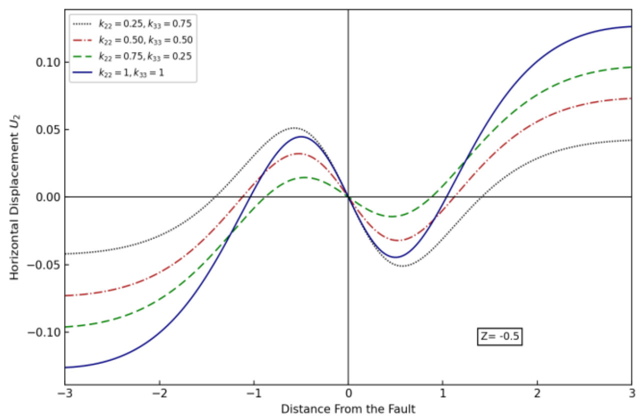

Figure 5 Variations of horizontal displacement U_2 due to a perfect and an imperfect interface in medium-I

As shown in Figure 5 shows U_2 in medium–I at Z = –0.5, again antisymmetric about the fault. Its amplitude is largest for the welded interface and diminishes with increasing imperfection, so that in medium–I both displacement components are attenuated by imperfect bonding. For this source, U_2 is an odd function of Y.

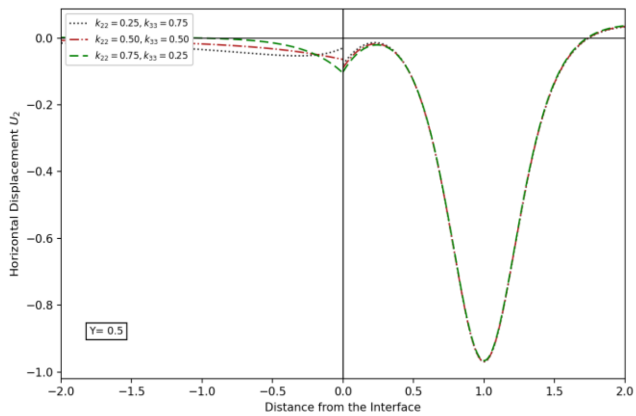

Figure 6 Discontinuity of horizontal displacement U_2 due to an imperfect interface

As shown in Figure 6 illustrates the discontinuity of U_2 across the interface at a fixed distance Y = 0.5 from the fault, with the medium–I branch (Z < 0) and the medium–II branch (Z > 0) plotted together. Because the bonding is imperfect, the two one–sided limits at Z = 0 do not coincide, and a finite jump appears, whose magnitude grows as the interface departs further from the welded state.

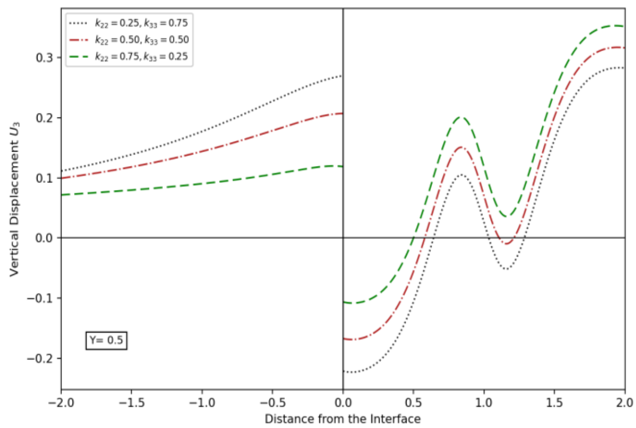

Figure 7 Discontinuity of vertical displacement U_3 due to an imperfect interface

As shown in Figure 7 shows the corresponding discontinuity of U_3, which is more pronounced: the displacement is positive on the medium–I side and jumps to negative values across the interface. This jump is the direct manifestation of the dislocation–like condition $u_i^{(I)} = [k_{ij}]\, u_j^{(II)}$, which permits a displacement discontinuity while keeping the

International Research Journal on Advanced Engineering and Management
https://goldncloudpublications.com
https://doi.org/10.47392/IRJAEM.2026.0390
e ISSN: 2584-2854
Volume: 04 Issue: 08
August 2026
Page No: 2741 - 2754

tractions continuous.

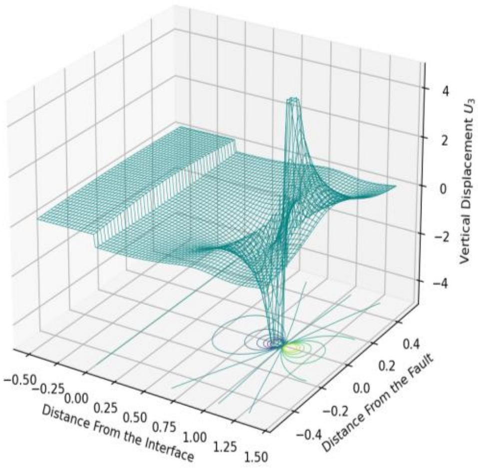

Figure 8 **3-D mesh grid map for dimensionless vertical displacement U_3**

As shown in Figure 8 is the three–dimensional mesh–grid map of U_3 over the (Y, Z) plane. The field is flat far from the fault, rises to a single dominant spike at the line source (Y = 0, Z = 1) where $R \to 0$, and steps across the interface plane Z = 0; the contour projection beneath the surface localises the deformation about the source.

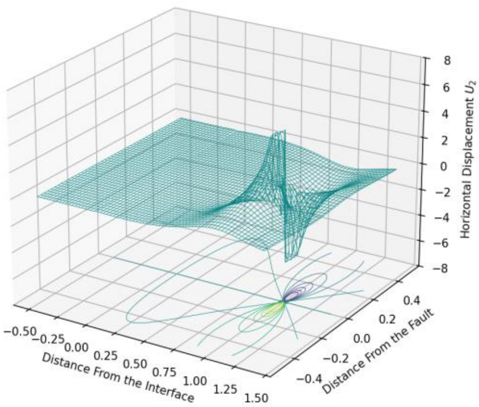

Figure 9 **3-D mesh grid map for dimensionless horizontal displacement U_2**

Figure 9 is the mesh–grid map of U_2, which exhibits the antisymmetric twin–lobe pattern (one positive and one negative lobe about Y = 0) consistent with the odd character of the horizontal displacement, together with the source spike and the step across the interface.

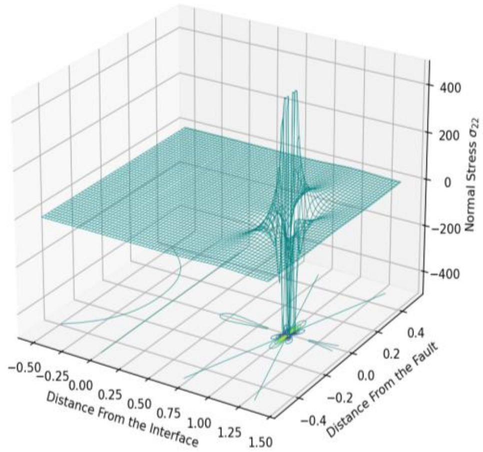

Figure 10 **3-D mesh grid map for the dimensionless normal stress σ_{22}**

Figure 10 shows the mesh–grid map of the dimensionless normal stress σ_{22}. Away from the fault, the stress is negligible; it develops a sharp twin (positive–negative) spike at the source, where the stresses are singular. In the dislocation–like model, σ_{22} is continuous across the interface — there is no step at Z = 0.

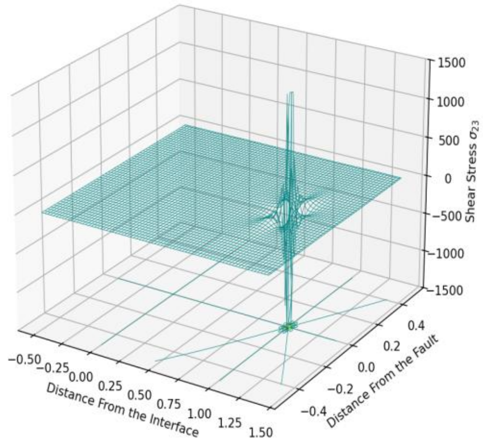

Figure 11 **3-D mesh grid map for the dimensionless shear stress σ_{23}**

As shown in Figure 11 gives the map of the shear stress σ_{23}, a single tall spike concentrated at the source that, like all the stress components, remains continuous across the interface.

e ISSN: 2584-2854
Volume: 04 Issue: 08
August 2026
Page No: 2741 - 2754

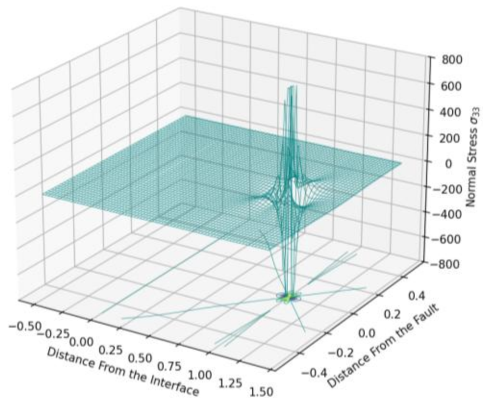

Figure 12 **3-D mesh grid map for the dimensionless normal stress σ_{33}**

As shown in Figure 12 shows the normal stress σ_{33}, a localised peak–and–well pair at the source that decays rapidly with distance and is continuous across the interface. Together, Figures 10–12 confirm that in the dislocation–like model the discontinuity resides in the displacements, not in the tractions. In addition to the above, many general observations emerge from Figures 2–12. First, the kinematic symmetry of the 45° source is opposite to that of the vertical dip–slip fault: the vertical displacement U_3 is an even (symmetric) function of the distance from the fault, forming a single trough in medium–II (Figure 2) and a single peak in medium–I (Figure 3) centred on $Y = 0$, whereas the horizontal displacement U_2 is an odd (antipodal–symmetric) function, forming the characteristic S–shape that vanishes at the fault (Figures 4 and 5). Second, the state of interface bonding controls the amplitude of the transmitted field: in medium–I both U_2 and U_3 are largest for the welded interface ($k_{22} = k_{33} = 1$) and are progressively reduced as the bonding weakens, so that imperfection attenuates the deformation carried into the upper half–space; in medium–II the three imperfect cases nearly coincide close to the fault and differ mainly in their far–field decay. The influence of interface imperfection on the displacements is therefore markedly stronger in medium–I than in medium–II.
Third, the discontinuity plots (Figures 6 and 7) show that imperfect bonding produces a finite jump in the displacements at the interface $Z = 0$, whose magnitude increases as the interface departs further from the welded state and is largest for the vertical component U_3; a perfectly welded interface would render these curves continuous. The three–dimensional mesh–grid maps (Figures 8–12) reinforce these observations and add two further points. The whole deformation field is strongly localised about the line source ($Y = 0$, $Z = 1$), where the displacements and — even more sharply — the stresses become singular and decay rapidly with distance in both media. In the dislocation–like model, the step across the interface plane appears only in the displacement maps (Figures 8 and 9); the stress maps (Figures 10–12) remain continuous across $Z = 0$, the normal stresses σ_{22} and σ_{33} forming twin and peak–and–well spikes and the shear stress σ_{23} a single dominant spike at the source. Collectively, the graphs confirm that, for a 45° dip–slip fault, interface imperfection redistributes and attenuates the displacement field — most strongly near the interface and within medium–I — while leaving the tractions continuous, in accordance with the dislocation–like bonding conditions.

Conclusion

The principal conclusions are:

- For the 45° source, the vertical displacement U_3 is symmetric (even) and the horizontal displacement U_2 is antisymmetric (odd) about the fault — the reverse of the vertical dip–slip fault.
- In medium–I the displacements are largest for the perfect interface and are systematically reduced as the bonding weakens, so that the deformation transmitted into the upper half–space is weakened by interface imperfection; in medium–II the bonding condition chiefly reshapes the far–field decay rather than the near–fault peak.
- Imperfect bonding produces a jump discontinuity in the displacements at the interface (Figures 6–9), whereas the stresses remain continuous across it (Figures 10–12); the displacement jump grows as the interface departs further from the welded state and is largest for the vertical component U_3.
- Both the displacement and the stress fields are strongly concentrated at the line source,

e ISSN: 2584-2854
Volume: 04 Issue: 08
August 2026
Page No: 2741 - 2754

where they become singular; the mesh–grid maps quantify how rapidly the field decays away from the source and how interface imperfection perturbs it. Since interfaces in the real Earth are seldom perfectly welded, the present imperfect–interface solution provides a more realistic description of how a 45° dip–slip rupture loads the surrounding crust than the classical welded–interface model.

Applications and future scope

In earthquake source modelling, oblique/45° dip–slip geometries are typical of many thrust and normal–faulting events, and the closed–form field provides a fast forward model for static displacements and stresses. In interpreting geodetic observations (GPS, InSAR and levelling), the predicted displacements can be fitted to measured coseismic and interseismic deformation to invert for fault slip, dip and depth, and — importantly — for the degree of bonding of subsurface interfaces. The two–medium model represents crust–mantle (Moho), sediment–basement or fault–gouge contacts, which are rarely welded, and thus quantifies how much displacement actually crosses such a contact. Further applications arise in reservoir and induced–seismicity geomechanics (hydrocarbon, geothermal, CO_2–storage and wastewater operations that reactivate dip–slip faults), in volcano–deformation and dam/reservoir–loading problems, and in the near–fault design of tunnels, pipelines, foundations and critical facilities. Mathematically, the same bimaterial–interface problem also describes load transfer across imperfectly bonded interfaces in layered composites and coatings. Several extensions merit future study. The present analysis may be generalised to an arbitrary dip angle δ so that the vertical (90°), the 45° and the horizontal (0°) faults appear as special cases of a single formulation, and to combined dip–slip–plus–tensile (mixed–mode) sources. The force–like interface, for which the tractions rather than the displacements jump, could be treated for the 45° source to complement the present dislocation–like results. The isotropic half–spaces may be replaced by orthotropic, monoclinic or transversely isotropic media, or by a layered (multi–interface) crustal model, and the elastic response may be extended to a viscoelastic one to capture post–seismic relaxation. Finally, coupling the analytic solution with real GPS/InSAR data sets in an inversion scheme would allow the bonding parameters (k_{22}, k_{33}) of actual crustal interfaces to be estimated from observed surface deformation.

References

[1]. Bala, N. and Rani, S. (2009). Static deformation due to a longburied dip–slip fault in an isotropic half–space welded with an orthotropic half–space. Sadhana, 34(6), 887–902.
[2]. Ben–Zion, Y. (1990). The response of two half–spaces to point dislocations at the material interface. Geophysical Journal International, 101(3), 507–528.
[3]. Chinnery, M.A. (1961). The deformation of the ground around surface faults. Bulletin of the Seismological Society of America, 51(3), 355–372.
[4]. Chu, H.J., Pan, E., Han, X., Wang, J. and Beyerlein, I.J. (2012). Elastic fields of dislocation loops in three–dimensional anisotropic bimaterials. Journal of the Mechanics and Physics of Solids, 60(3), 418–431.
[5]. Dundurs, J. and Hetényi, M. (1965). Transmission of force between two semi–infinite solids. Journal of Applied Mechanics, 32(3), 671–674.
[6]. Fan, H. and Wang, G.F. (2003). Screw dislocation interacting with imperfect interface. Mechanics of Materials, 35(10), 943–953.
[7]. Freund, L.B. and Barnett, D.M. (1976). A two–dimensional analysis of surface deformation due to dip–slip faulting. Bulletin of the Seismological Society of America, 66(3), 667–675.
[8]. Garg, N.R., Madan, D.K. and Sharma, R.K. (1996). Two–dimensional deformation of an orthotropic elastic medium due to seismic sources. Physics of the Earth and Planetary Interiors, 94(1–2), 43–62.
[9]. Heaton, T.H. and Heaton, R.E. (1989). Static

International Research Journal on Advanced Engineering and Management
https://goldncloudpublications.com
https://doi.org/10.47392/IRJAEM.2026.0390
e ISSN: 2584-2854
Volume: 04 Issue: 08
August 2026
Page No: 2741 - 2754

deformations from point forces and force couples located in welded elastic Poissonian half–spaces: implications for seismic moment tensors. Bulletin of the Seismological Society of America, 79(3), 813–841.

[10]. Kumar, A., Singh, S.J. and Singh, J. (2005). Deformation of two welded elastic half–spaces due to a long inclined tensile fault. Journal of Earth System Science, 114(1), 97–103.

[11]. Kumari, A. and Madan, D.K. (2021a). Deformation field due to seismic sources with imperfect interface. Journal of Earth System Science, 130(4), 224.

[12]. Kumari, A. and Madan, D.K. (2021b). Deformation due to dip–slip and tensile faults in force–like imperfectly bonded elastic half–spaces. ISET Journal of Earthquake Technology, 58(2), 61–81.

[13]. Kumari, A. and Madan, D.K. (2024). Strike–slip dislocation in two imperfectly coupled orthotropic elastic half–spaces. International Journal of Applied and Computational Mathematics, 10, Article 32.

[14]. Madan, D.K. and Kumari, A. (2022). Stresses and displacements for two imperfectly joined half–spaces induced by a vertical tensile fault. Proceedings of the Indian National Science Academy, 88(1), 104–115.

[15]. Maruyama, T. (1964). Statical elastic dislocations in an infinite and semi–infinite medium. Bulletin of the Earthquake Research Institute, 42, 289–368.

[16]. Mindlin, R.D. (1936). Force at a point in the interior of a semi–infinite solid. Physics, 7(5), 195–202.

[17]. Okada, Y. (1985). Surface deformation due to shear and tensile faults in a half–space. Bulletin of the Seismological Society of America, 75(4), 1135–1154.

[18]. Rani, S. and Singh, S.J. (1992). Static deformation of a uniform half–space due to a long dip–slip fault. Geophysical Journal International, 109(2), 469–476.

[19]. Rani, S., Singh, S.J. and Garg, N.R. (1991). Displacements and stresses at any point of a uniform half–space due to two–dimensional buried sources. Physics of the Earth and Planetary Interiors, 65(3–4), 276–282.

[20]. Rongved, L. (1955). Force interior to one of two joined semi–infinite solids. Proceedings of the Second Midwestern Conference on Solid Mechanics, 1–13.

[21]. Savage, J.C. (1966). Surface deformation associated with dip–slip faulting. Journal of Geophysical Research, 71(20), 4897–4904.

[22]. Singh, S.J. and Garg, N.R. (1986). On the representation of two–dimensional seismic sources. Acta Geophysica Polonica, 34(1), 1–12.

[23]. Singh, S.J., Rani, S. and Garg, N.R. (1992). Displacements and stresses in two welded half–spaces caused by two–dimensional sources. Physics of the Earth and Planetary Interiors, 70(1–2), 90–101.

[24]. Singh, K., Madan, D.K., Goel, A. and Garg, N.R. (2005). Two–dimensional static deformation of an anisotropic medium. Sadhana, 30(4), 565–583.

[25]. Steketee, J.A. (1958). On Volterra's dislocations in a semi–infinite elastic medium. Canadian Journal of Physics, 36(2), 192–205.

[26]. Wu, W., Lv, C., Xu, S. and Zhang, J. (2017). Elastic field due to dislocation loops in isotropic bimaterial with dislocation–like and force–like interface models. Mathematics and Mechanics of Solids, 22(5), 1190–1204.

[27]. Yu, H.Y. (1998). A new dislocation–like model for imperfect interfaces and their effect on load transfer. Composites Part A, 29(9–10), 1057–1062.